Molecular Crystals and Liquid Crystals

ISSN: 1542-1406 (Print) 1563-5287 (Online) Journal homepage: http://www.tandfonline.com/loi/gmcl20

Aggregation property and photovoltaic performance optimization of symmetrical squaraine dye containing bis-anchoring groups for dye-sensitized solar cell

Yong Hui Lee, Ji Youn Kang, Dong Woo Kim, Ji Seon Kim, Jae Hong Kim & Thogiti Suresh

To cite this article: Yong Hui Lee, Ji Youn Kang, Dong Woo Kim, Ji Seon Kim, Jae Hong Kim & Thogiti Suresh (2016) Aggregation property and photovoltaic performance optimization of symmetrical squaraine dye containing bis-anchoring groups for dye-sensitized solar cell, Molecular Crystals and Liquid Crystals, 635:1, 148-157, DOI: 10.1080/15421406.2016.1200400

To link to this article: http://dx.doi.org/10.1080/15421406.2016.1200400

Published online: 01 Nov 2016.

MOLECULAR CRYSTALS AND LIQUID CRYSTALS
2016, VOL. 635, 148–157
http://dx.doi.org/10.1080/15421406.2016.1200400

Taylor & Francis
Taylor & Francis Group

Aggregation property and photovoltaic performance optimization of symmetrical squaraine dye containing bis-anchoring groups for dye-sensitized solar cell

Yong Hui Lee, Ji Youn Kang, Dong Woo Kim, Ji Seon Kim, Jae Hong Kim, and Thogiti Suresh

Department of Chemical Engineering, Yeungnam University, Gyeongsan, Gyeongbuk, Republic of Korea

ABSTRACT

The effect of chenodeoxycholic acid (CDCA) used as the coadsorbent with a symmetrical squaraine (SSQ) sensitizer on TiO_2-based solar cells was investigated, and it was found that the coadsorbent retards the SSQ sensitizer from aggregating on the TiO_2 photoanode but diminishes dye amount leading to an interdependent solar cell performance. Analysis of the optical spectra and incident photon-to-current conversion efficiency data revealed that the amount of SSQ sensitizer as well as the presence of aggregates is significantly dependent on the molar concentration of CDCA coadsorbent. In addition, electrochemical impedance and stepped light-induced transient measurements of photocurrent and voltage measurements are also used to explain and support the behavior of the co-sensitized solar cells. The short-circuit current density and open circuit voltage of the devices with CDCA increases due to the decreased charge transfer resistance, enhanced diffusion length and electron lifetime in the mesoporous TiO_2 photo electrode.

KEYWORDS

Dye-sensitized solar cell, squaraine dye, chenodeoxycholic acid, dye aggregation, electron diffusion length

Introduction

Dye sensitized solar cells (DSSCs) are considered to be efficient photovoltaic devices as a low-cost alternative to commercial Si-based solar cells [1, 2], because of the simple manufacturing process, colorful and transparent characters. A typical DSSC is constructed with a dye-absorbed semiconductor photo-electrode, an electrolyte containing I^-/I_3^- redox couples, and a Pt-coated counter electrode [3–6]. The photon-to-current conversion mechanism of DSSCs is based on the injection of electrons from the excited dye onto the conduction band of semiconductor photo-electrode. The oxidized dye molecules are reduced by electron injection from the electrolyte.

Among them, the dye plays an important role in injecting electrons onto the conduction band of the semiconductor electrode. Therefore, to produce a highly efficient solar cell, the dye molecules should absorb and convert a wide range of wavelengths in the solar spectrum. Since the incident photon-to-current efficiency (IPCE) of a solar cell is the product of the light harvesting efficiency for photons with wavelength λ (LHE(λ)), quantum efficiency of electron injection onto the conduction band of the semiconductor oxide (Φ_{inj}), the efficiency for dye

CONTACT Thogiti Suresh sureshyu@ynu.ac.kr
Color versions of one or more of the figures in the article can be found online at www.tandfonline.com/gmcl.

regeneration (η_{reg}), the and electron collection efficiency of the photo-generated charge carriers (η_{cc}), as shown in Eq. (1)[7].

$$\text{IPCE}(\lambda) = \text{LHE}(\lambda) \cdot \Phi_{inj} \cdot \eta_{reg} \cdot \eta_{cc} \quad (1)$$

The most successful photosensitizing dye molecule for DSSCs are ruthenium polypyridyl complexes (Ru-complex), which yield solar-to-electric power conversion efficiencies of 9–11% under AM 1.5 G, 100 mW/cm^2 light illumination [8–10]. However, it contains the ruthenium metal ion which is an expensive precious metal species that increases the cost of DSSCs. The Ru-free organic dye structure has been studied extensively due to their ease of synthesis, high molar extinction coefficients and variable structure modifications [11–17].

Among the various Ru-free organic dyes, squaraine (SQ) dyes have attracted considerable interest due to the higher molar extinction coefficients than conventional dyes. They can also absorb photons with a long wavelength in the range, 500∼700 nm [18–20]. Although it is well known that SQ dyes tend to aggregate on the TiO_2 surface which reduces the solar cell performance, it will be great challenge to develop SQ dye and optimize the cell performance for the production of high performance DSSCs.

We had reported the photovoltaic property of the symmetrical SQ (SSQ) dye containing bis-anchoring groups in a molecule [17] which revealed the enhanced charge transfer character between SQ dyes and TiO_2 electrode to compare with that of mono-anchored SQ dyes. In this paper, we investigated the aggregation properties in solution state and TiO_2 adsorbed solid state of SSQ dyes which were considered in terms of the photovoltaic performance in DSSCs. IPCE and electrochemical impedance spectroscopy (EIS) analyses were also performed to study and optimize the interfacial electron transfer process in DSSCs. Meanwhile, we also studied the electron lifetime and diffusion length parameters by using stepped light-induced transient measurements of photocurrent and voltage (SLIM-PCV) analysis.

Experiment details

Materials

All commercially available starting materials and solvents were purchased from Aldrich, TCI, and ACROS Co. and were used without further purification unless otherwise stated. The synthesis for squarine dye used in this study was followed with known method [17], and molecular structure of symmetrical squarine (SSQ) dye was shown in Fig. 1.

Assembly and characterization of DSSCs

The transparent conducting glass substrates were cleaned with ethanol, DI water and acetone with ultrasonication, respectively. The TiO_2 pastes were prepared using ethyl cellulose (Aldrich), Lauric acid (Fluka, City, State, Country), and Terpineol (Aldrich). The TiO_2 particles used were ca. 20 – 30 nm in diameter. The prepared TiO_2 paste was doctor-bladed onto the pre-cleaned glass substrates, followed by calcination at 500°C for 30 min then drying at 70°C. The scattering layer consisting of rutile TiO_2 particles (250 nm in a size) was deposited onto the mesoporous TiO_2 films. These layers were dipped in an aqueous solution of $TiCl_4$ (0.04 M) at 70°C for 30 min. TiO_2 layers were immersed in the SSQ dye solutions containing different molar concentrations of CDCA for 24 h.

The Pt counter electrodes were prepared by thermal reduction of the films dip-coated in H_2PtCl_6 (7.0 mM) in 2-propanol at 400°C for 20 min. The dye-adsorbed TiO_2 and Pt counter

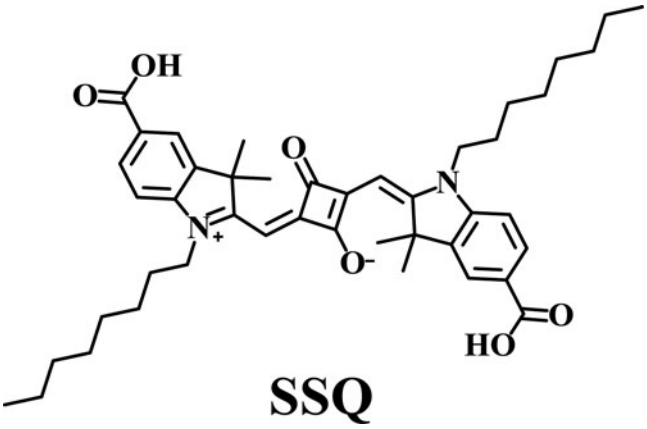

Figure 1. Chemical structure of SSQ dye.

electrodes were sandwiched between 60 m-thick Surlyn (Dupont 1702), used as a bonding agent and spacer. Through a pre-punched hole on the Pt counter electrode, liquid electrolyte (I^-/I_3^- redox couple) was then introduced and finally sealed. The active area of the dye-adsorbed TiO_2 films was estimated using a digital microscope camera with image-analysis-software (Moticam 1000).

The photocurrent-voltage measurement was performed using a Keithley model 2400 Source Meter and a Newport 91192 solar simulator system (equipped with a 1 kW xenon arc lamp, Oriel). Light intensity was adjusted to 1 sun (100 mW/cm^2) with a Radiant Power Energy Meter (model 70260, Oriel). The incident photon-to-current conversion efficiency (IPCE) results were acquired from IPCE G1218a (PV Measurement). This system applies monochromatic light from a 75 W xenon arc lamp (Ushio UXL-75XE) filtered by a dual-grafting monochromator and individual filters onto the test devices. An ellipsoidal reflector collects light from the lamp and focuses on the monochromatic entrance slit via a mechanical chopper to create a small modulated signal. While the modulated, monochromatic light was applied to the test devices, a continuous bias light (ca. 1 sun) was also applied. Electrochemical impedance spectroscopy (EIS) was performed using an electronic-chemical analyzer (Iviumstat Tec.).

Transient measurements were performed by a same method to O'Regan et al. [21] and as illustrated elsewhere [22]: a white light bias was generated from an array of diodes (Abet, LS Series light source) with red-light pulsed diodes (Thorlabs HNL210L system) as the perturbation source, controlled by a fast solid-state switch. The voltage dynamics were measured on a 1 GHz Tektronix oscilloscope (DPO4102B-L) across the high impedance (1 MΩ) port. The perturbation light source was set to a suitably low level such that the voltage decay kinetics were mono-exponential. Small perturbation transient photocurrent measurements were performed in a similar manner to the open-circuit voltage decay measurement. For the voltage decay measurements in the short-circuit regime, a Keithley 2600B source meter was connected in series with the solar cell and parallel with the oscilloscope which was set on the high impedance port. The Keithley sourced the current through the solar cell which was under bias illumination in such a way that the voltage was kept at 0 V (i.e., short-circuit). In this way no extra current is allowed to flow through the device following the light pulse, therefore the decay of the measured perturbation signal is entirely governed by the charge recombination within the cell. For the current decay measurements, while the charge is being collected the charges are also simultaneously recombining within the cell.

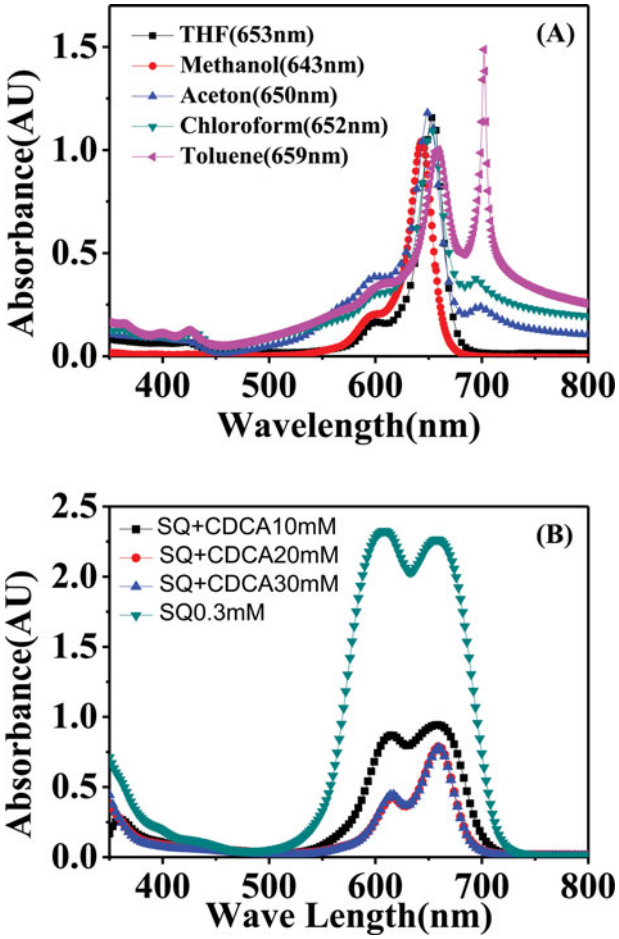

Figure 2. UV-Vis absorption spectra of SSQ dye in the solution state (A), and on the TiO_2 absorbed solid state (B).

Results and discussion

The SSQ dye can easily aggregates in the solution and solid state which can be well detected in the UV-Vis absorption spectrum as their blue shifted H-aggregate form (600 nm) and the red shifted J-aggregate form (695 nm) to compare with that of monomeric form (653 nm) in the solution state. The cause for the pronounced shift in absorption is the rather high transition dipole moment of squaraine molecule [23, 24]. In accordance with the molecular exciton theory, this causes a large splitting of the excitonic states upon the interaction of the transition dipoles [23]. Which type of aggregate is formed, depends solely on the arrangement of the transition dipoles relative to the molecule axis. In the H-aggregation, the transition dipole of molecules is arranged with opposite direction between the planar structures that causes a hypsochromic shift in the absorption spectra. However the parallel arrangement of transition dipoles promotes a bathochromic shift compared to that of the monomeric state of SQ dye.

In order to study the issue of aggregation, the absorption of SSQ-dye was measured in different solvents (Fig. 2a) and sensitized films without and with different molar concentration of CDCA coadsorbent (Fig. 2B). The position and shape the of the absorption pattern changed with respective to the solvent. In high polar solvents such as MeOH, a single absorption peak with a weak short wavelength shoulder is detected. Hence, less aggregation occurs in high

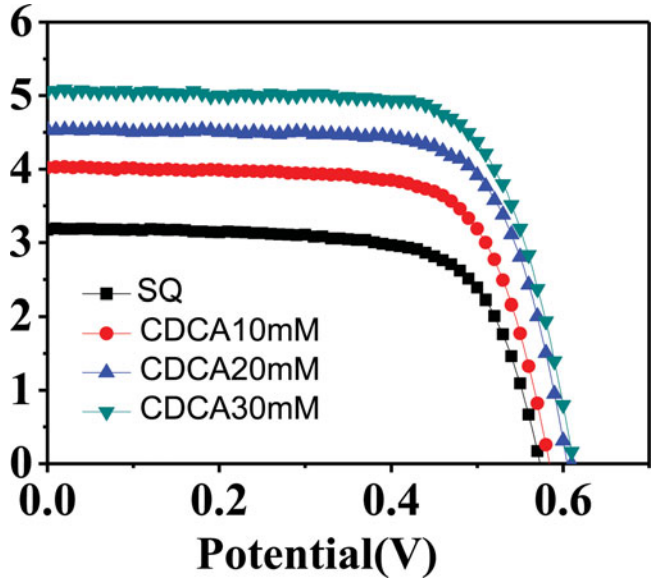

Figure 3. Current-voltage characteristics for DSSCs containing SSQ dyes with co-adsorbent CDCA (AM 1.5 G, 100mW/cm^2).

polar solvents. In less polar solvents like toluene spectrum shows an intense main absorption band (653 nm with shoulder at 610 nm) and a stronger long wavelength band (700 nm). UV-Vis spectra of the SSQ sensitized TiO_2 film without CDCA (Fig. 2B), exhibiting a broadened absorption spectrum as well as a new peak around 600 nm, which is due to aggregation of SSQ. This new absorption band is assigned as due to H-aggregates on TiO_2 film. The extent of H-aggregation of SSQ can be estimated by comparing the ratio of the optical density of the aggregate band (AH, 600 nm) and the monomer band (AQ, 640 nm) on TiO_2 films sensitized with SSQ dye. A high value of the ratio, AH/AQ, indicates a large extent of H-aggregation of SSQ. AH/AQ of the SSQ stained TiO_2 film without CDCA was 1.02, while the ratio decreased to 0.91 and 0.56 with the addition of CDCA to the dye solutions and coadsorbed onto the TiO_2 surface. Hence, the CDCA in SSQ solution diminished the aggregation of the SSQ dye onto the TiO_2 surface when coadsorbed with CDCA coadsorbent. The aggregation is generated during the adsorption process in the dye solution, and hence it can be avoided by the presence of CDCA on the TiO_2 surface because CDCA adsorbs competitively with SSQ sensitizer. A decrease in the Q-band peak in the presence of CDCA was mainly caused by reduced SSQ loading on the TiO_2 surface.

It is well known that the aggregation of photosensitizers causes the decrease of photo-injection from the exited sensitizer to photoelectrode due to the energy loss in their aggregated state which reduces the J_{SC} value in the DSSC. Furthermore, the aggregates of photosensitizers can act as the site for the recombination of the electron that is injected from the exited photosensitizers onto the surface of the photoelectrode. Therefore, the coadsorbent CDCA is usually used to reduce the aggregation of photosensitizers on the photoelectrode. Neale N. R. et al. reported that the adsorbed CDCA reveal not to have an effect on the charge injection efficiency from the excited sensitizer to photoelectrode [25].

Figure 3 presents the photovoltaic performance of the DSSCs sensitized by SSQ dye with and without CDCA and corresponding cell performance parameters depicted in Table 1. From the Table 1 and Figure 3, DSSC sensitized by SSQ without CDCA, a short circuit photocurrent density (J_{SC}) of 3.18 mA cm^{-2} was obtained under standard solar conditions (global AM 1.5).

Table 1. Photovoltaic parameters of DSSCs.

Sample	J_{SC}(mA/cm^2)	V_{OC}(V)	FF	ŋ(%)	Amount of dye (mol/cm^2)
SQ	3.18	0.57	0.71	1.27	7.20×10^{-8}
CDCA10mM	4.54	0.60	0.70	1.94	2.76×10^{-8}
CDCA20mM	5.07	0.61	0.70	2.15	1.60×10^{-8}
CDCA30mM	6.30	0.62	0.69	2.69	0.64×10^{-8}

Under similar conditions in the presence of 10 mM CDCA in the dye solution, a photocurrent enhancement from 3.18 to 4.54 mA cm^{-2} was achieved. Upon increasing the CDCA concentration to 20 and 30 mM, the photocurrent further increased to 5.07 and 6.30 mA cm^{-2}. On the other hand, the open circuit voltage also increased with increasing CDCA concentration. The highest efficiency of 2.69% was achieved with 30 mM CDCA.

In order to look into the effect of CDCA on dye loading, the concentration of SSQ dye was calculated after desorbing the sensitizer from the photoelectrode film and followed by calculation with the Beer–Lambert law [26]. The amount of SSQ sensitizer adsorbed onto the TiO_2 surface was decreased with increasing concentration of CDCA, when compared to the SSQ dye in the absence of CDCA (Table 1). However, the photocurrent did not decrease proportionally with the dye loading of SSQ (Fig. 4). As we discussed above the adsorbed CDCA do not have an effect on charge injection efficiency, and thus the retardation of charge injection by CDCA is not taken into account [25]. The enhanced J_{SC} can presumably arise from diminished aggregation of SSQ dye following high light harvesting in the Q-band region [27]. In addition, a relatively low coverage of SSQ sensitizer is presumably sufficient to absorb a large fraction of photons because of the high molar extinction coefficient of SSQ. Also, we can gain a higher open circuit voltage from an increased concentration of CDCA.

Figure 5 shows the incident photon-to current conversion efficiency (IPCE) as a function of molar concentration of CDCA coadsorbent. The IPCE values increased with increasing CDCA molar concentration and this could be attributed to the low extent of aggregated SSQ molecules. A broadening in the IPCE at no or a low extent of CDCA was shown, but it decreased with increasing CDCA concentration. The IPCE data unravels the effect of CDCA on aggregation, confirming that the CDCA adsorbed with SSQ onto the TiO_2 surface reduces the aggregation of the sensitizer.

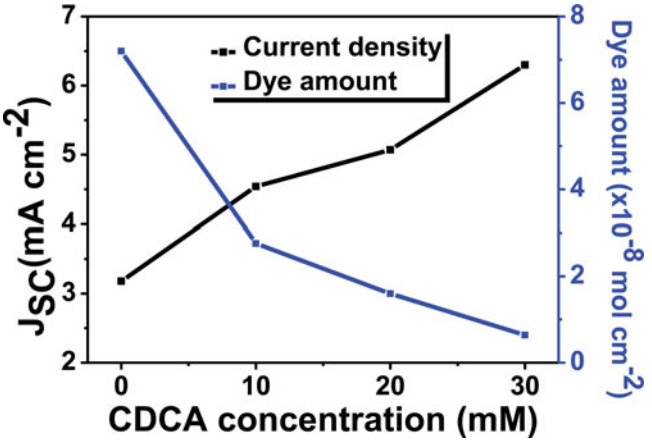

Figure 4. Increasing and decreasing rates current density and dye amount vs. CDCA concentration.

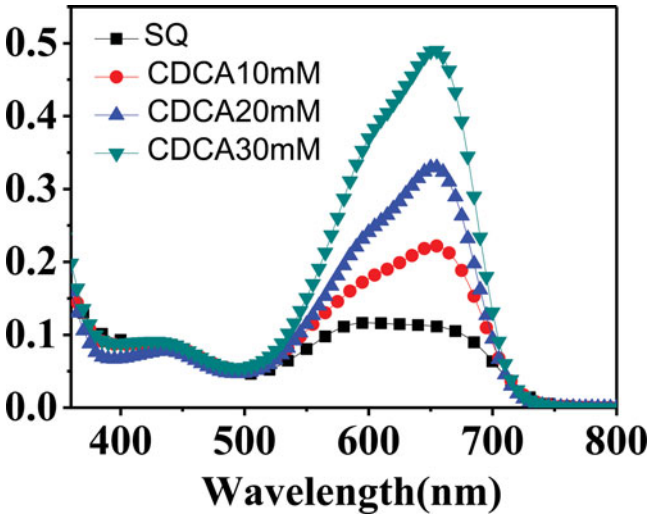

Figure 5. IPCE curves for DSSCs containing SSQ dyes with co-adsorbent CDCA.

Electrochemical impedance spectroscopy (EIS) technique was used to study the charge transfer resistances of the cells. Fig. 6 shows the EIS data of the DSSCs sensitized with and without CDCA, and the equivalent circuit is shown inside Fig. 6. The fitting is done by using Z-View software and the fitting lines are included in Fig. 6 and resistances listed in the Table 2. The smaller and larger semicircles in the Nyquist plots were attributed to the charge transfer at the counter electrode/electrolyte interface and the TiO_2/dye/electrolyte interface, respectively. R1 is the series resistance, R2 is the resistance of electron transport in the counter electrode and R3 is the electron transfer resistance between the TiO_2 film and electrolyte. Smaller R3 values of 34.32, 29.85, and 27 Ω was obtained for the DSSC sensitized by a dye solution containing 10, 20, and 30 mM CDCA, respectively as compared to that of the cell sensitized by a dye solution without CDCA (37.79 Ω). The higher R3 of the DSSC without CDCA is due to the dye aggregation on the TiO_2 film. The effectiveness of CDCA in preventing dye aggregation is supported by performing EIS analyses. It is generally accepted that CDCA can prevent

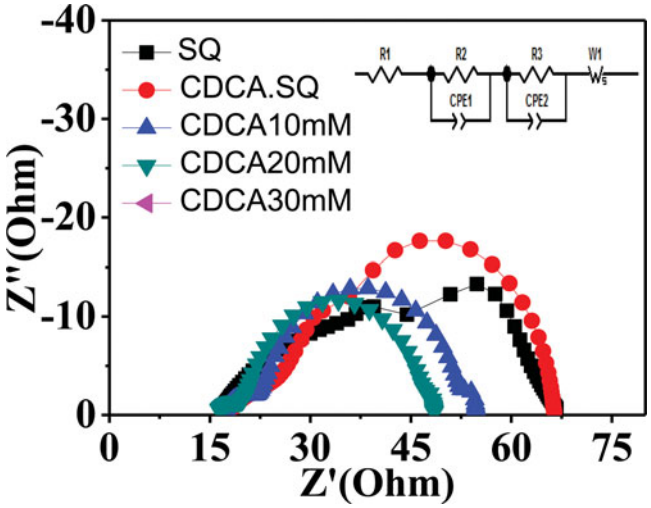

Figure 6. Nyquist plots of DSSC at the light illumination.

Table 2. Electrochemical impedance parameters of DSSCs.

Sample	R1[a)]	R2[b)]	R3[c)]
SQ	16.28	9.17	37.79
CDCA10mM	17.55	12.46	34.32
CDCA20mM	16.99	5.90	29.85
CDCA30mM	15.96	4.43	27.00

[a)]: FTO Interface resistance.
[b)]: Resistance at the interface between the counter electrode and electrolyte.
[c)]: Resistance originated from the backward charge transfer from TiO_2 to the electrolyte and the electron conduction in TiO_2 electrode.

dye aggregation and thereby decrease the charge transfer resistance (R3) at the surface. The decrease of R3 with CDCA is consistent with the result depicted in Fig. 3.

The parameters electron lifetime (τ_e), electron diffusion coefficient (D_n) and electron diffusion length (L_n) extracted from the stepped light-induced transient measurements of photocurrent and voltage (SLIM-PCV) (Figure 7 and Table 3) are crucial parameters (3) for the

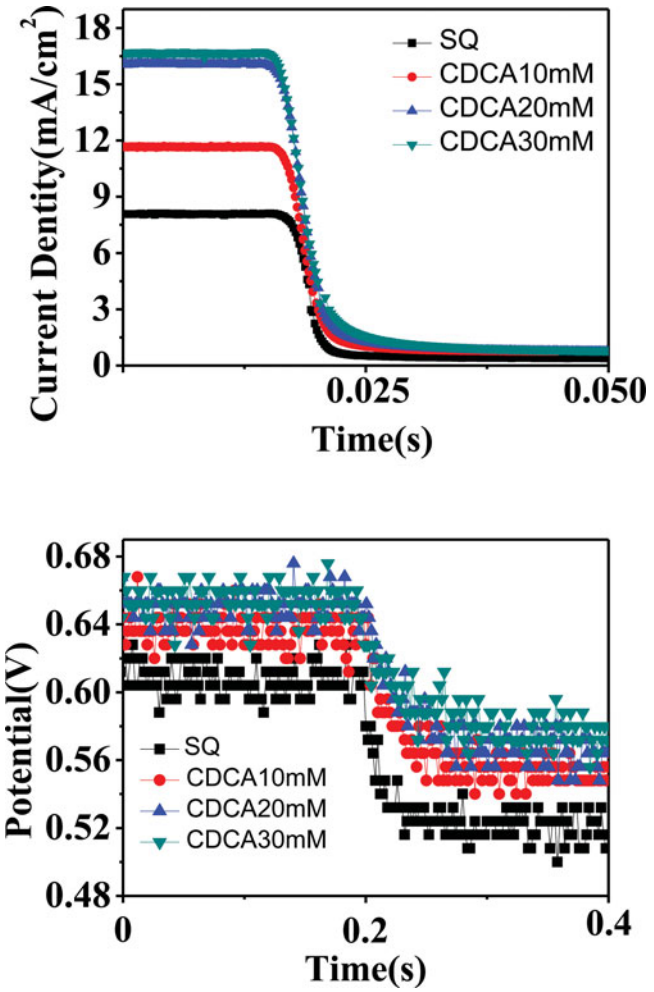

Figure 7. (a) Typical current responses of DSSCs against the different stepped laser intensities; (b) Typical open circuit voltage transients induced by stepped laser intensity.

Table 3. SLIM-PCV analysis at different CDCA concentrations.

Sample	D_n(cm^2/s) (Electron Diffusion Coefficients)	τ_e(s) (Electron Lifetime)	L_n(μm) (Electron Diffusion Length)
SQ	0.000050	0.036	13.42
CDCA10mM	0.000056	0.056	17.71
CDCA20mM	0.000059	0.068	19.51
CDCA30mM	0.000061	21.25	0.074

efficient working of dye solar cell. The electrodes immersed into dye solution containing different extent of CDCA show a longer lifetimes, compared to the lifetime of the electrode without CDCA. The order of the above lifetime values is consistent with that of the V_{OC} trend. Therefore, the increased electron lifetime may be the intrinsic reason for the increased V_{OC} values of the DSSCs based on devices with CDCA compared to that for device without CDCA. Moreover, the obtained electron diffusion coefficient values for DSSCs by SSQ dye with different extent of CDCA are larger than DSSC sensitized by SSQ dye without CDCA, which suggest that the electron can travel more through the TiO_2 matrix in case of devices with CDCA coadsorbent. The electron diffusion length (L_n) is a useful tool to reflect the electron collection efficiency. Higher L_n values were obtained for devices containing 10, 20 and 30 mM of CDCA, which are longer than the thickness of the TiO_2 film. As the L_n increase, chances of charge separation at TCO surface increase leading to higher electron collection efficiency.

Conclusions

The effect of chenodeoxycholic acid as the coadsorbent with symmetrical squaraine sensitizer was investigated for the dye sensitized solar cell application. Co-adsorbed CDCA on mesoporous TiO_2 reduces the SSQ sensitizer's loading, but diminishes the H-aggregation onto TiO_2 as seen from the absorption and IPCE spectral data. The reduced dye loading did not affect the photocurrent. Advantageously, the incorporation of CDCA enhances the charge transfer process. The measurement of the stepped light induced transient analysis showed that the presence of CDCA with SSQ on the TiO_2 surface induced not only an improved electron lifetime but also increases the diffusion length in the TiO_2 electrode. As a result, the photovoltage and photocurrent density of the cells with chenodeoxycholic acid is higher when compared to the cell without chenodeoxycholic acid.

Acknowledgments

This work was supported by "Human Resources Program in Energy Technology" of the Korea Institute of Energy Technology Evaluation and planning (KETEP), granted financial resource from the Ministry of Trade, Industry & Energy, Republic of Korea. (No. 20154030200760).

References

[1] O'Regan, B., Grätzel, M. (1991). *Nature*, *353*, 737.
[2] Grätzel, M. (2001). *Nature*, *338*, 414.
[3] Chiba, Y., Islam, A., Watanabe, Y., Komiya, R., Koide, N., , Y., Han, L. (2006). *Jpn. J. Appl. Phys.*, *45*, L638.
[4] Gao, F., Wang, Y., Shi, D., Zhang, J., Wang, M. K., Jing, X. Y., Humphry-Baker, R., Wang, P., Zakeeruddin, S. M., Grätzel, M. (2008). *J. Am. Chem. Soc.*, *130*, 10720.
[5] Cao, Y. M., Bai, Y., Yu, Q. J., Cheng, Y. M., Liu, S., Shi, D., Gao, F. F., Wang, P. (2009). *J. Phys. Chem. C.*, *113*, 6290.

[6] Nazeeruddin, M. K., Zakeeruddin, S. M., Humphry-Baker, R., Jirousek, M., Liska, P., Vlachopoulos, N., Shklover, V., Fischer, C.-H., Grätzel, M. (1999). *Inorg., Chem.*, *38*, 6298.
[7] Zhang, G., Bala, H., Cheng, Y., Shi, D., Lv, X., Yu, Q., Wang, P. (2009). *Chem. Commun.*, 2198.
[8] Gao, F. F., Wang, Y., Shi, D., Zhang, J., Wang, M. K., Jing, X. Y., Humphry-Baker, R., Wang, P., Zakeeruddin, S. M., Grätzel, M. (2008). *J. Am. Chem. Soc.*, *130*, 10720.
[9] Yu, Q., Wang, Y., Yi, Z., Zu, N., Zhang, J., Zhang, M., Wang, P. (2010). *ACS Nano*, *4*, 6032.
[10] Ozawa, H., Sugiura, T., Shimizu, R., Arakawa, H. (2014). *Inorg. Chem.*, *53*, 9375.
[11] Horiuchi, T., Miura, H., Sumioka, K., Uchida, S. (2004). *J. Am. Chem. Soc.*, *126*, 12218.
[12] Wang, Z. S., Cui, Y., Hara, K., Dan-Oh, Y., Kasada, C., Shinpo, A. (2007). *Adv. Mater.*, *19*, 1138.
[13] Kim, M. S., Cho, M. J., Choi, Y. C., Ahn, K.-S., Choi, D. H., Kim, K., Kim, J. H. (2013). *Dyes Pigments*, *99*, 986.
[14] Hara, K., Sato, K., Katoh, R., Furube, A., Ohga, Y., Shinpo, A. (2003). *J. Phys. Chem. B.*, *107*, 597.
[15] Hwang, S., Lee, J. H., Park, C., Lee, H., Kim, C., Park, C. (2007). *Chem. Commun.*, 4887.
[16] Park, S. S., Won, Y. S., Choi, Y. C., Kim, J. H. (2009). *Energ. Fuels*, *23*, 3732.
[17] Lee, C. H., Yun, H. J., Jung, M. R., Lee, J. G., Kim, S. H., Kim, J. H. (2014). *Electrochim. Acta*, *138*, 148.
[18] Chen, G., Yokoyama, D., Sasabe, H., Hong, Z. R., Yang, Y., Kido, J. (2012). *Appl. Phys. Lett.*, *101*, 4.
[19] Law, K. Y. (1993). *Chem. Rev.*, *93*, 449.
[20] Law, K. Y., Bailey, F. C. (1992). *J.Org. Chem.*, *57*, 3278.
[21] O'Regan, B., Lenzmann, F. (2004). *J. Phys. Chem. B.*, *108*, 4342.
[22] Snaith, H. J., Humphry-Baker, R., Chen, P., Cesar, I., Grätzel, M. (2008). *Nanotechnology*, *19*, 424003.
[23] Deing, K. C., Mayerhöffer, U., Würthner, F., Meerholz, K. (2012). *Phys Chem Chem Phys.*, *14*, 8328.
[24] Yesudas, K., Chaitanya, G. K., Prabhakar, C., Bhanuprakash, K., Rao, V. J. (2006). *J. Phys. Chem. A.*, *110*, 11717.
[25] Neale, N. R., Kopidakis, N., Van de Lagematt, J., Graetzel, M., Frank, A. J. (2005). *J. Phys. Chem. B.*, *109*, 23183.
[26] Lu, H., Deng, K., Shi, Z., Liu, Q., Zhu, G., Fan, H., Li, L. (2014). *Nanoscale Res. Lett.*, *9*, 183.
[27] Yum, J. H., Jang, S. R., Humphry-Baker, R., Graetzel, M., Cid, J. J., Torres, T., Nazeeruddin, M. K. (2008). *Langmuir*, *24*, 5636.